NANOSYSTEMS: PHYSICS, CHEMISTRY, MATHEMATICS, 2014, 5 (5), P. 650–658

# OPTICAL MICRO-STRUCTURING OF METAL FILMS ON THE SURFACE OF DIELECTRIC MATERIALS: PROSPECTS OF SHAPING BY NON-DIFFRACTING OPTICAL BEAMS

R. Drampyan[1,2], T. Vartanyan[3]

[1]Institute for Physical Research, National Academy of Sciences of Armenia, 0203, Ashtarak-2, Armenia

[2]Armenian - Russian (Slavonic) University, H. Emin str. 123, 0051, Yerevan, Armenia

[3]National Research University of Information Technologies, Mechanics and Optics, St. Petersburg, Russia

rafael.drampyan@gmail.com, Tigran.Vartanyan@mail.ru

**PACS 32.80.Lg, 34.50.Dy, 81.16.Mk**

The technique of optical micro-structuring of metal films based on processes of metal atoms adsorption on the surface of crystalline substrate and simultaneous controllable photo-stimulated desorption of atoms by non-uniform laser beam illumination is presented. The experiments were performed for sodium atom deposition on a sapphire substrate. The sapphire substrate was illuminated through a commercial linear mire with a pitch of 10 $\mu$m by a 440 nm laser beam with 1W/cm$^2$ intensity. This provides the nonuniform spatial distribution of the illumination intensity over the sapphire surface and optical control of sodium atom deposition on the sapphire substrate, preventing the nucleation and growth of the granular film in the illuminated areas. Experiments showed that the mire pattern was well reproduced in the sodium deposits, thus creating the microstructured metallic film with few tens nm thickness. The novel suggestion to use nondiffracting optical beams for high contrast microstructuring of surface metal film is presented.

**Keywords:** metal nanoparticle, adsorption, desorption, laser controlled growth, non-diffracting optical beams.

*Received: 19 August 2014*

## 1. Introduction

Planar micro- and nanophotonic devices are the subject of burgeoning area of research because of the wide usage of applications in optoelectronics and photonics. These uses include display devices, sensors, optical communication systems, nano-photonic devices, metamaterials etc.

Among the different technologies to manufacture metallic, semiconductor or organic nanostructures, *top-down* technologies are the most prevalent [1,2]. They include molecular beam epitaxy, mask and interference photolithography, as well as electron beam lithography.

Planar technologies for producing device structures for research in the domain of metamaterials, photonic crystals and nano-photonics were reviewed in [3-5]. Electron beam lithography (EBL) remains the most powerful method for the generation of lithographic patterns in the mentioned domain due to the combination of high precision, better than 50 nm, and programmability. EBL is relevant also as a pattern generator for the masks used in

deep ultra-violet lithography. In spite of many advantages the EBL technique requires very expensive equipment and long processing times.

In this respect, *bottom-up* technologies also have merit. These technologies are based on self-organized and photoinduced formation of nanostructures [6,7]. However, the resulting topology is rather irregular.

An attractive possibility for producing metal nanoparticles is light-induced atomic desorption as a tool for controlling the surface atom density of the adsorbed atoms during the physical vapor deposition process. Such experiments were started in the 1990's from pioneering work [8]. The physics of the process is based on the fact that strong enough nonuniform illumination diminishes the density of the adsorbed atoms in illuminated areas below a threshold value necessary for initiation of the nucleation process. Thus, the deposition pattern reproduces the spatial distribution of the illumination intensity over the surface. The adsorbtion-desorption experiments were performed with the use of alkali metal (Na, Rb, Cs) atoms in different works (see [8-13], and references therein) and Zn and Sn in [14]. The deposition of silver on a silver chloride single crystal and silver adatom absorption spectrum has been studied in [15]. Analogous experiment with deposition of gold atoms on the amorphous silica was performed in [16].

The nonuniform light beam can be obtained by mask or interference techniques. In [11] the nonuniform light beam was obtained by illumination of the substrate through the cooper wire greed with a pitch of 100 $\mu$m. In [13], in order to create a metallic grating, the spatial profile of a laser beam was modulated with reflection from a Fresnel mirror. The feasibility of the interference technique to produce surface structures with a pitch of 260 nm was substantiated in [10].

In this paper we present the results of adsorption and deposition of sodium atoms on the sapphire substrate and optical control of film deposition with the use of a mire with a pitch of 10 $\mu$m.

We suggest also the use of the non-diffracting beams, particularly Bessel beams for the formation of micrometer-scale spatially modulated beams. Exposing of the atomic deposits on the substrate surface with periodically or quasiperiodically spatially modulated non-diffracting beams is advantageous, since the light intensity distribution is stable in the course of beam propagation, providing high contrast of the metallic micro- and nanostructured patterns. The experimental formation of zero$^{th}$ order Bessel beam by an axicon is presented.

## 2. Spectroscopy of the adsorbed atoms

The schematic for atom adsorption on the surface of the dielectric material is shown in Fig.1. Such atoms are commonly called adatoms. In some cases, the structure of the electronic levels changes dramatically, such that the adatom looses its similarity to the free atom at all.

The experimental realization of adsorption was performed with the use of a specially designed spectroscopic cell. To enhance the adatom absorption, 17 polished sapphire plates were introduced in the cell that was evacuated and filled with sodium. The cell design allows independent control of the sapphire plates' temperature and the sodium vapor density. The latter was achieved through the variation of the temperature of the metal drop placed in an appendix attached to the cell. The standard experiment run consists of absorption spectra registration at the fixed cell temperature and variable temperature of the appendix. Absorption due to the free sodium vapor was measured in a separate cell with the same optical length and subtracted. The spectra were obtained with the use of standard "Perkin-Elmer" spectrometers and are shown in Fig.2.

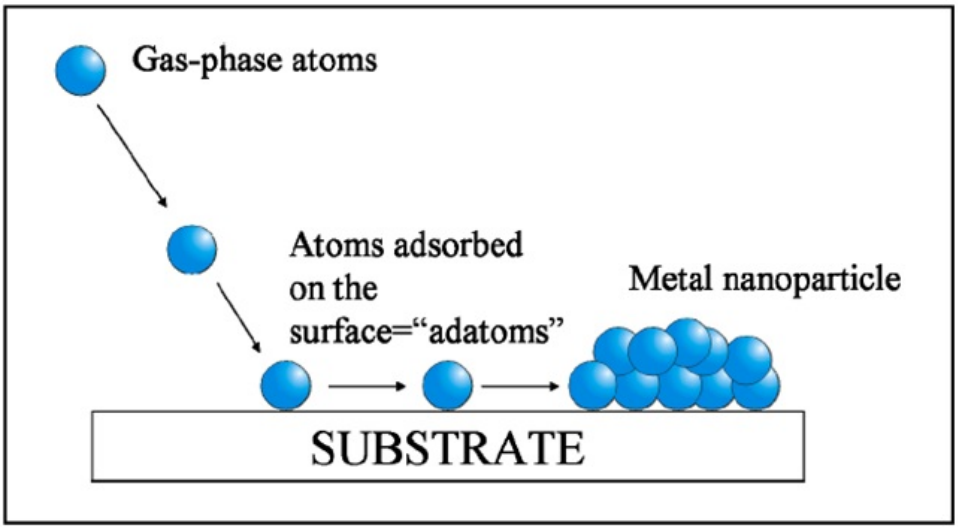


FIG. 1. Schematic of adsorbtion of atoms and nanoparticle formation on a dielectric surface

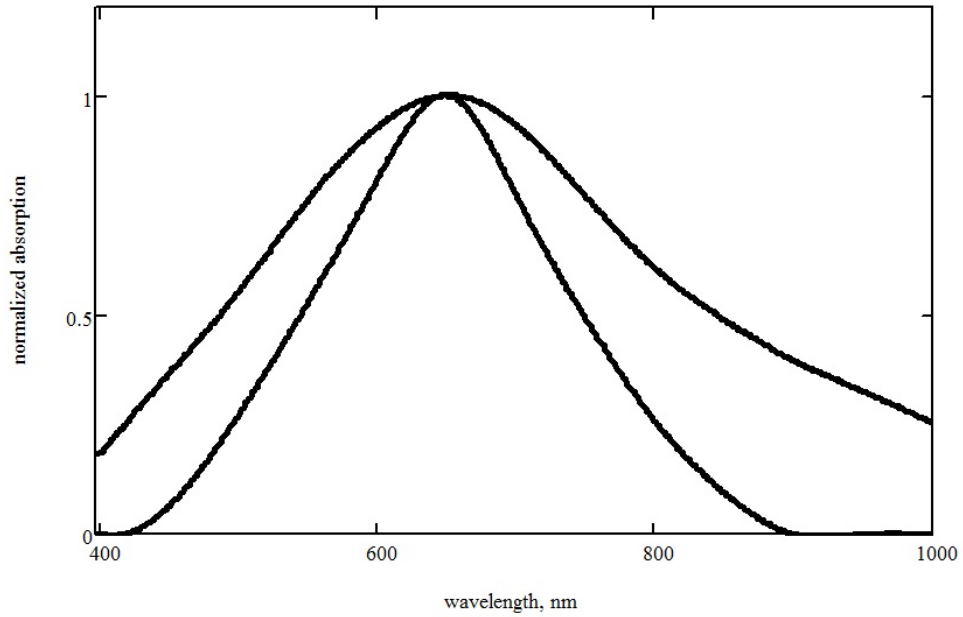


FIG. 2. Absorption spectra of sodium adatoms on the surface of sapphire kept at 470 K (narrow curve) and 670 K (broader curve). The spectra were normalized to facilitate the comparison of the broadening due to the temperature rise

Optical absorption of this system is dominated by a broad structureless band (Fig.2), somewhat shifted to the red from the position of the characteristic yellow doublet of free sodium at 589 nm. The absorption cross section of the atom at the maximum $\sigma$ was found to be equal to $3 \times 10^{-16}$ cm$^2$ while the integral of the absorption cross section over the wavelength corresponds nicely to the oscillator strength of the corresponding transition in the free atom.

These measurements proved that sodium atoms are adsorbed on the sapphire surface in atomic form and preserve their identity.

## 3. Photodesorption process

The photodesorption process is a very promising tool for direct laser writing of complicated patterns on surfaces. Although an ordinary heating of the substrate by absorbed radiation can cause thermal desorption of adsorbed species from the illuminated area, nonthermal mechanisms of desorption attracts much more attention. The reasons for that are higher spatial resolution, higher selectivity as well as lower inertia of nonthermal process as compared to thermal ones.

The illumination of the adsorbed atoms on the surface of the substrate can lead to photon absorption either by the substrate or by the adsorbed species. In the latter case, electronic excitation of an adatom is transformed into its motion away from the surface.

One particular example of such a process is photodesorption of sodium atoms from sapphire. Sapphire is transparent to visible light, while the adsorbed sodium atoms, as was detailed in the previous section, possess a broad absorption band in this spectral range. The nonthermal nature of sodium photodesorption from sapphire was proved in [14]. More details of the process were reported in [8]. Fig.3 shows the concept for the desorption experiment and the registration scheme. Optical methods provide high sensitivity, which allows for sure registration of the atoms desorbed with different velocities in one laser shot of 10 ns duration.

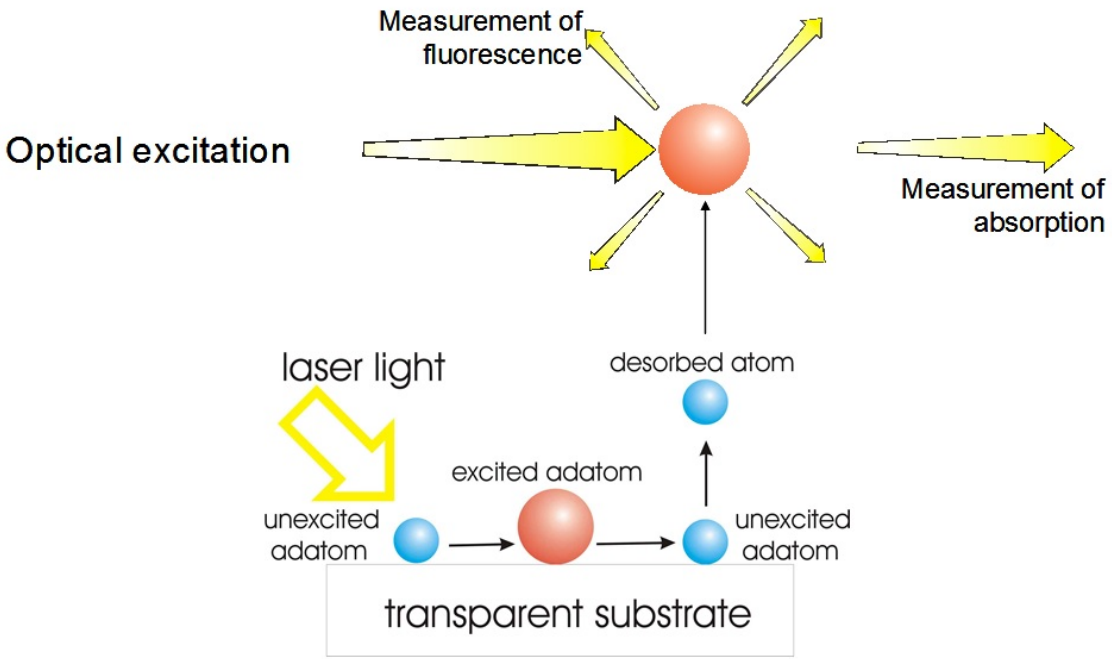


FIG. 3. Registration of photodesorption via absorption or fluorescence measurements

Fig.4 plots the photodesorption spectrum and contrasts it with the absorption spectrum already given in Fig.2. Although the maxima of the two spectra almost coincide, quantum efficiency of desorption diminishes for larger wavelengths and drops to zero at 800 nm. This threshold corresponds to the photon energy of 1.55 eV. It is in excess of the binding energy of adatoms $E_{ad}$=0.7 eV, which was deduced from the temperature dependence of absorption spectrum.

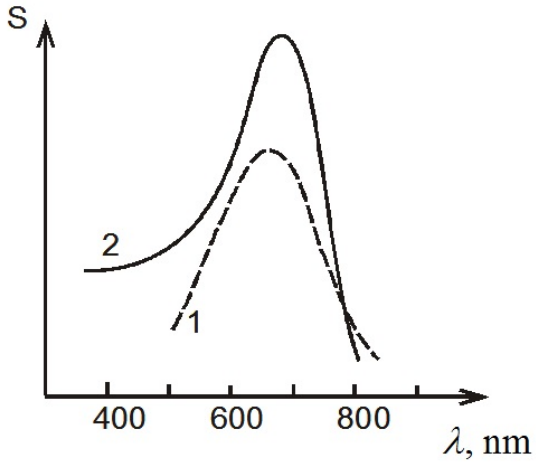


FIG. 4. Absorption (1) and photodesorption (2) spectra of individual sodium atoms adsorbed on the sapphire surface. The ordinate scale is given in arbitrary units

## 4. Estimation of light intensity for controllable film deposition

As was mentioned before, strong enough nonuniform illumination diminishes the number density of the adsorbed atoms in the illuminated areas below the threshold value necessary for the initiation of the nucleation process.

Estimations of light beam critical intensity, I required for the elimination of formation of metallic layer in illuminated area can be performed with the use of the following formula:

$$I = \alpha \frac{\hbar\omega}{\tau\sigma w f} \tag{1}$$

derived in [17] based on the balance equitation for surface density $n$ of atoms for the adsorption-desorption process under illumination by nonuniform light at photon energy $\hbar\omega$. The other notations in formula (1) are as follows: $\alpha$ is the adhesion coefficient of a metal atom to the clean substrate admitted to be of the order of 0.01, $\tau = 1$ s is the characteristic time required to form a metal monolayer in the dark spaces, $w$ is the photodesorption quantum yield measured in [8] to be equal to 0.001 provided the light wavelength is within absorption band of adsorbed atoms, and $f$ is the critical surface concentration of adsorbed atoms that gives rise to the nucleation of metallic phase taken to be 0.01 of atomic monolayer. Substituting these values and the energy of photon $\hbar\omega$=2 eV in formula (1) one can obtain the value of critical intensity 3 W/cm$^2$.

## 5. Laser control for sodium metallic film deposition

In many cases, it is desirable to pattern granular metal films. Photodesorption of metal atoms from the surface of transparent dielectric materials may be used to obtain regular arrays of metal nanoparticles [10]. Illumination of the substrate during physical vapor deposition reduces the density of the atoms adsorbed on the surface, thus precluding nucleation and growth of the granular film in the illuminated areas [8,14].

We report here on the results of experiments performed with sodium deposition on sapphire. The threshold intensity of a cw diode laser operated at the wavelength of 440 nm was found to be 1 W/cm$^2$ for a deposition rate of 0.02 nm/s. The substrate was illuminated through the mire with a pitch of 10 $\mu$m. The microscopic images of the sodium deposits as

well as the image of the mire are presented in Fig.5. The deposition takes place at the dark sites on the cell window. The mire pattern was shown to be well reproduced in the sodium deposits.

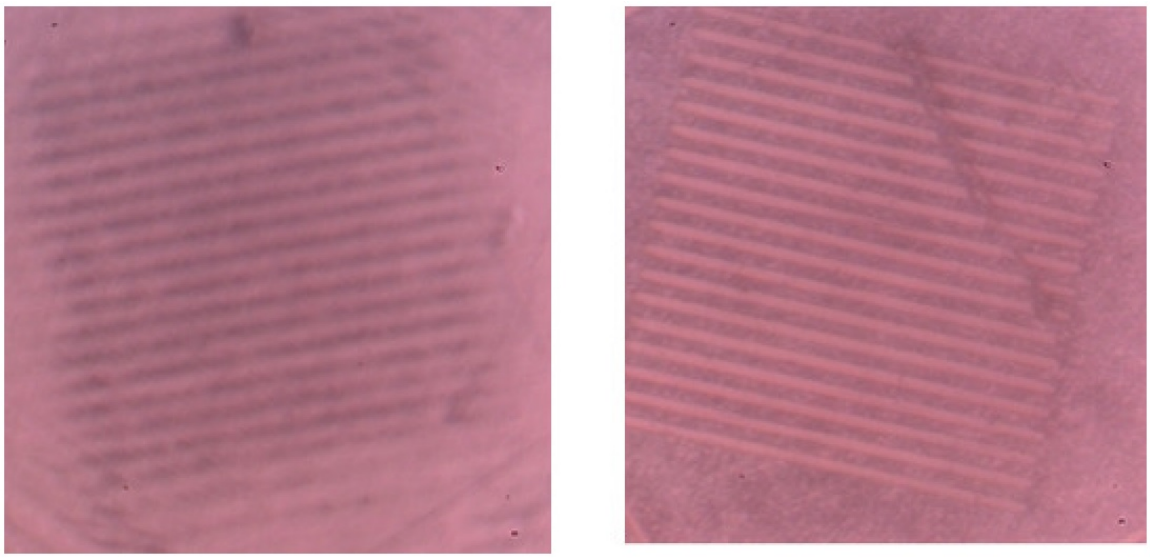

FIG. 5. (a) microscopic image of the sodium deposits on sapphire substrate obtained via physical vapor deposition under simultaneous laser illumination through the mire with 10 $\mu$m periodicity shown in (b)

Further reduction of the pitch can be achieved with an interference technique [10]. More promising is the use of non-diffracting beams providing high contrast of the metallic micro- and nanostructured patterns.

## 6. Prospects of the use of non-diffracting beams

Non-diffracting optics is a very active area of research in the field of optical beams and their applications. The diffraction-free beams have a feature of conserving their transverse intensity distribution during propagation in free space [18,19]. The simplest diffraction free beams can be formed by superposition of plane waves, whose wave vectors lie on the cone. The zero$^{th}$ order Bessel beam is a particular case of diffraction-free beams. The profile of the Bessel beam is a set of concentric rings. The envelope of intensity profile of Bessel beam decreases inversely proportional to the radial distance [18]. A number of practical ways to generate Bessel beams have been suggested, including the use of ring apertures [18], Fabry-Perot interferometers [20], programmable phase modulators based on the phase-imprinting technique [21], holographic diffractive elements [22] and nonlinear generation of conical emission [23]. One of the ways to form Bessel beams is the use of optical element – axicon [24]. Bessel beams have numerous applications, for example, for optical manipulation of micro-sized objects, optical tweezers (see [25] and references therein), formation of Bessel like photonic lattices in photorefractive materials [26] etc.

### 6.1. Formation of Bessel beam by an axicon

Bessel beam formation by an axicon used in our experiments is shown schematically in Fig.6. The laser source was the Thorlabs HRP-170 single mode He-Ne laser at 633 nm operation wavelength, with 17 mW power and beam diameter of 0.7 mm. The linearly polarized Gaussian beam was expanded by confocal lenses (Fig.6a). The Gaussian beam

after passing through the axicon (Del Mar Photonics AX-BK-7-175) with aperture cone angle 175°, was transformed to the Bessel beam (Fig.6b). The convergence angle of the beams behind the axicon was adjusted by moving the output lens of the beam expander back or forth, thus varying the convergence angle within ∼4–2°, which in turn changes the spacing between the concentric rings in the range of 10–20 $\mu$m. The distance along Z axis where the converging beams are overlapped and form the Bessel beam (Fig.1a,c) was measured $Z_{max}$ ∼10 cm. The spacing between the concentric rings, measured by beam profiler, shows their equidistant disposition, except for a few central rings. The period of annular structure shown in the Fig.6b was measured by beam profiler Thorlabs BP109-VIS and was 10 $\mu$m for certain position of output lens of beam expander. The beams become divergent behind the overlapping zone $Z_{max}$, forming a ring pattern (Fig.6c).

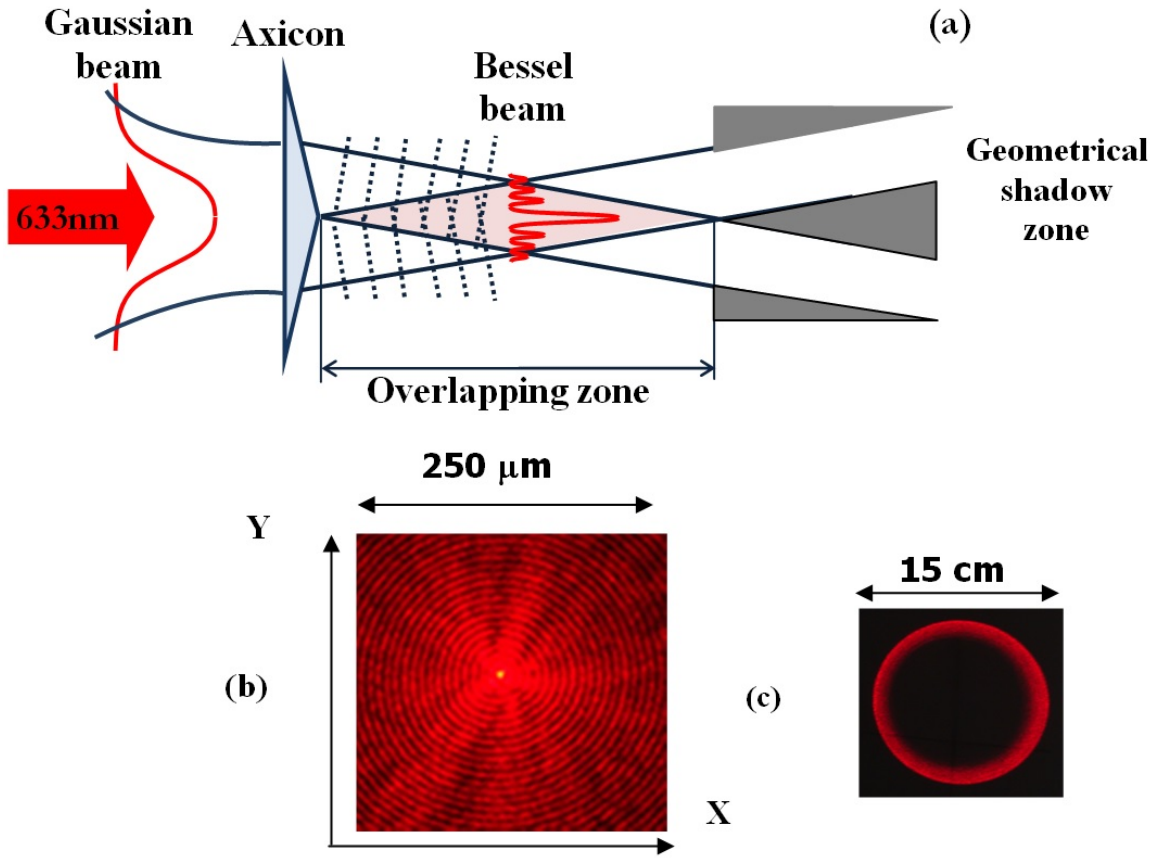


FIG. 6. (a) Experimental scheme illustrating the formation of Bessel beam by an axicon. (b) Fragment of transverse intensity distribution of Bessel beam formed by an axicon with aperture cone angle 175° in the overlapping zone of the beams. The number of rings reaches up to 500. (c) Ring pattern at the distance of 2 m behind the overlapping zone, where the beams become divergent

A Bessel beam can be formed similarly for a 100 mW cw 532 nm laser beam, which is suitable for deposition control in Na and Rb atomic vapor cells.

Exposing of the atomic deposits on the substrate surface with periodically or quasiperiodically modulated non-diffracting beams is advantageous, since the light intensity distribution is stable in the course of beam propagation [18], providing high contrast of the metallic

micro- and nanostructured pattern. These experiments are in progress and will be published elsewhere.

The technique developed for exposing of the atomic deposits by Bessel beams can be extended to other types of nondiffracting beams such as Airy [27], first order Bessel [28] and Mathieu and Weber [29] beams.

## 7. Conclusion

The technique of optical shaping of surface metallic micro- and nanostructures based on metal atom adsorption processes on the surface of crystalline substrate and simultaneous controllable photostimulated desorption of atoms by nonuniform laser beam illumination is presented. The experiments were performed for sodium atom deposition on a sapphire substrate. The absorption spectra of adatoms, as well as desorbed atoms are measured. The manufacturing of a micrometer-scale metal grid was performed with the use of a mire with 10 $\mu$m pitch. The novel suggestion to use nondiffracting Bessel optical beams for high contrast microstructuring of surface metal film and the formation of zero$^{th}$ order Bessel beam by an axicon are presented.

The suggested techniques open new possibilities for the laser structuring of the metal films with micrometric resolution. The structured metal films have a number of applications in fast and sensitive photo-detection [30], high performance photovoltaics [31], subwavelength metal gratings and polarizers [32], surface enhanced Raman scattering [33], surface second harmonic generation [34-37] etc.

## Acknowledgments

The financial support from EU project LIMACONA (IRSES-GA-2013-6126000) and from Government of Russian Federation (Grant 074-U01) is gratefully acknowledged.

## References

[1] S.Y.Lin, J.G.Flemming, D.C. Hetherington et al. *Nature*, **394**, P. 251 (1998).
[2] Y.W.Su, C.S.Wu, C.C.Chen, C.D.Chen. *Advanced Materials*, **15** P. 49 (2003).
[3] N.P. Jonson, R.M. De La Rue, S.A.De La Rue, "Metamaterials at Optical Frequencies: Fabrication and Measurements" in Applications of Metamaterials, CRC Press. Ed. F. Capolino, Chapter 30 (2009).
[4] S.Linden, "Fabrication and Optical Characterization of Photonic Metamaterials" in Applications of Metamaterials, CRC Press. Ed. F. Capolino, Chapter 29 (2009).
[5] Richard De La Rue et al, "Planar nanophotonic devices in integration technologies" in Photonics and Micro- and Nano-structured materials, Ed. Rafael Drampyan, Proc. of SPIE, Vol. **8414**, P. 841402 (2012).
[6] A. Arsenault, et al, *J. Mater. Chem.* **14**, P. 781 (2004).
[7] X.Wang et al. *Adv. Mater.*, **17**, P. 2103 (2005).
[8] A.M. Bonch-Bruevich, T.A. Vartanyan, A.V.Gorlanov, Yu.N. Maksimov, S.G. Przhibrlskii, V.V.Khromov. Photodesorption of sodium from the surface of sapphire. *Sov. Phys. JETP*, **70**, P. 604–608 (1990).
[9] T.A.Vartanyan et al. "Photoexitation and photoregistration of atomic motion on the surfaces of solid materials", in New Trends in Quantum Coherence and Nonlinear Optics", Editor, R.Drampyan, Nova Science Publishers, NY, P. 245–263 (2009).
[10] T.A.Vartanyan, V.V. Khromov, N.B. Leonov, S.G. Przhibelskii, "Shaping of surface nanostructures via non-termal light-induced process", in Fundamentals of Laser-Assisted Micro- and Nanotechnologies 2010, Edited by P.Veiko , T.A. Vartanyan, Proc. SPIE, Vol.**7996**, P. 7996OH 1-7 (2011).
[11] T.A. Vartanyan et al, "Granular metal films on the surfaces of transparent dielectric materials studied and modified via optical means", in Photonics and Micro- and Nano-structured Materials 2011, Edited by Rafael Drampyan, Proc. SPIE, Vol. **8414**, P. 841404 1-7 (2012).

[12] C. Marinelly, A.Burchianti, A.Bogi, F. Della Valle, G.Bevilacqua, E.Mariotti, S.Veronesi, L.Moi. Desorption of Rb and Cs from PDMS induced by nonresonant light scattering, *Eur. Phys. D*, **37**, P. 319–325 (2006).
[13] A.E.Afanasyev, P.N. Melentyev, V.I. Balykin. Quantum adsorbtion of atoms on the surface induced by laser light, *Pis'ma Zh. Eks.Teor Fiz.*, **86**, P. 198–203 (2007).
[14] I.N.Abramova, E.B.Aleksandrov, A.M.Bonch-Bruevich, V.V.Khromov. Photostimulated desorption of metal atoms from surface of transparent insulator, *JETP Letters*, **39**, P. 203–205 (1984).
[15] A.N.Latishev, O.V.Ovchinnikov, S.S. Okhotnikov. *J.Appl.Spectr.*, **70**, P. 817–820 (2003).
[16] J.-M. Antonietti, M.Michalski, U.Heiz, H.Jones, K.H.Lim, N. Roesch, A.D.Vitto, G. Pacchioni, *Phys. Rev Lett.*, **94**, P. 213402 (2005).
[17] T.A. Vartanyan, V.V.Khromov, N.B.Leonov, S.G. Przhibelskii. Optical methods for formation of metallic nanostructures on the surface of dielectric materials, *Opticheskii Zhournal*, **78**(8), P. 47–50 (2011).
[18] J. Durnin, J.J. Mikely Jr, J.H. Eberly. Diffraction-free beams. *Phys. Rev. Lett.*, **58**, P. 1499–1501 (1987).
[19] V. Bagini, F. Frezza, M. Santarsiero, G. Schettini, G. Spagnolo. Generalized Bessel-Gauss beams, *J. Mod. Optics*, **43**, P. 1155–1166 (1996).
[20] A.J. Cox and D.C. Dibble. Nondiffracting beams from a spatially filtered Fabry–Perot resonator, *J. Opt. Soc. Am. A*, **9** P. 282–286 (1992).
[21] N. Chattrapiban, E.A. Rogers, D. Cofield, W.T. Hill, III, and R. Roy. Generation of nondiffracting Bessel beams by use of a spatial light modulator. *Opt. Lett.*, **28**, P. 2183–2185 (2003).
[22] J. Turunen, A. Vasara, and A. T. Friberg. Holographic generation of diffraction-free beams. *Appl. Opt.*, **27** P. 3959–3962 (1988).
[23] R.Drampyan. Formation of diffraction-free beams by laser generation of conical emission in a Kerr medium. *Appl. Phys.B*, **68**, P. 77–79 (1999).
[24] Shafer F. P. On some properties of axicons. *Appl. Phys. B*, **39**, P. 1-8 (1986).
[25] J. Arlt, V. Garces-Chavez, W. Sibett, K.Dholakia. Optical micromanipulation using a Bessel light beam. *Opt Commun.*, **197**, P. 239 (2001).
[26] A. Badalyan, R. Hovsepyan, P. Mantashyan, V. Mekhitaryan, R. Drampyan. Bessel standing wave technique for optical induction of complex refractive lattice structures in photorefractive materials. *J. Modern Optics*, **60**, P. 617–628 (2013).
[27] P.Rose, F. Diebel, M. Boguslawski, C. Denz. Airy beam induced optical routing. arXiv:1202.5724.v1 [physics. optics] 26 Feb 2012.
[28] J. Arlt, K. Dholakia. Generation of high-order Bessel beams by use of an axicon. *Optics Commun.*, **177**, P. 297–301 (2000).
[29] P. Rose, M. Boguslawski, C. Denz. Nonlinear lattice structures based on families of complex nondiffracting beams. *New J. Phys.*, **14**, P. 033018. (2012).
[30] D. M. Schaadt, A. B. Feng, and E. T. Yub. Enhanced semiconductor optical absorption via surface plasmon excitation in metal nanoparticles. *Appl. Phys. Lett.*, **86**, P. 063106 (2005).
[31] D. Derkacs, W. V. Chen, P. M. Matheu, S. H. Lim, P. K. L. Yu, and E. T. Yu. Nanoparticle-induced light scattering for improved performance of quantum-well solar cells. *Appl. Phys. Lett.*, **93**, P. 091107 (2008).
[32] Seh-Won Ahn, Ki-Dong Lee, Jin-Sung Kim, Sang Ho. Fabrication of a 50 nm half-pitch wire grid polarizer using nanoimprint lithography. *Nanotechnology*, **16**, P. 1874–1877 (2005).
[33] Paul L. Stiles, Jon A. Dieringer, Nilam C. Shah, Richard P. Van Duyne. Surface-enhanced Raman spectroscopy. *Annual Review of Analytical Chemistry*, **1**, P. 601–626 (2008).
[34] M. Ishifuji, M. Mitsuishi, T. Miyashita. Bottom-up design of hybrid polymer nanoassemblies elucidated plasmon-enhanced second harmonic generation from nonlinear optical dyes. *J.Am.Chem, Soc.*, **131**, P. 4418–4424 (2009).
[35] Yu. Zhang, N. K. Grady, C. Ayala-Orozco, N. K. Halas. Three-dimensional nanostructures as high efficient generator of second harmonic light. *Nano Lett.*, **11**, P. 5519–5523 (2011).
[36] J. Fuitowski et al. Mapping of gold nanostructure-enhanced near fields via laser scanning second harmonic generation and ablation. *Journal of Nanophotonics*, **6**, P. 063515 (2012).
[37] M.Centini, A.Benedetti. Second harmonic generation in plasmonic nanoresonators. *Journal of Nanophotonics*, **7**, P. 078501 (2013).